VNU Journal of Science: Comp. Science & Com. Eng., Vol. 42, No.3 (2026) 69-86

VNU Journal of Science:
Computer Science and Communication Engineering

Journal homepage: http://www.jcsce.vnu.edu.vn/index.php/jcsce

Original Article

# Personalizing Federated Learning based on Adapting Representation Learning for Anomaly Detection in Home Health Monitoring Systems

Ly Vu*, Trung Tin Nguyen

*Le Quy Don Technical University, Hanoi, Vietnam*

Received 27th January 2026
Revised 06th April 2026; Accepted 18th May 2026

**Abstract:** The proliferation of Internet of Things (IoT) wearable devices has enabled real-time human activity recognition for home health monitoring, including fall detection. However, deploying machine learning models in these scenarios faces challenges from data privacy concerns and the non-Independently and Identically Distributed (non-IID) nature of sensor data across users. Federated learning (FL) addresses privacy by enabling collaborative training without centralized data collection, but existing FL frameworks struggle with data heterogeneity. We propose FL based on Adaptive Local Training (FedALT), where each client's model consists of an Autoencoder (AE) for learning latent representations and a Predictor (PD) for classifying activities, including abnormal actions such as falls. The key innovation is the Adaptive Local Training (ALT) mechanism, which dynamically adjusts the contribution of global and local AE models during local initialization using only the unsupervised RE loss, thereby mitigating bias caused by non-IID label distributions. Experiments on three wearable sensor datasets, i.e., MobiAct, MobiFall, and HAR, demonstrate that FedALT consistently outperforms existing FL frameworks, particularly in classifying minority and abnormal action classes under heterogeneous data distributions.

*Keywords:* Anomaly Detection, Federated learning, IoT

## 1. Introduction

The rise of Internet of Things (IoT) devices, e.g., wearable devices, has unlocked unprecedented opportunities for real-time human activity recognition, with applications ranging from healthcare monitoring (e.g., fall detection for elderly care) to personalized fitness tracking [1–3]. However, deploying machine learning models in such scenarios faces two critical challenges. First, data privacy constraints as raw IoT sensor data from wearable devices often contain sensitive user information [4–6]. Second, the data is usually

*Corresponding author.
*E-mail address:* vu.ly@lqdtu.edu.vn

https://doi.org/10.25073/2588-1086/vnucsce.6867

distributed as non-Independently and Identically Distributed (non-IID) distributions, where sensor data patterns vary widely across users due to differences in device placement, user behavior, and environmental conditions [7, 8]. Federated learning (FL) offers a privacy-preserving solution by enabling collaborative model training without centralized data collection [5, 6, 9]. However, existing FL frameworks struggle to adapt to the inherent heterogeneity of wearable data, often resulting in suboptimal performance for activity classification, particularly for minority classes such as fall actions that are critical in health monitoring applications [10, 11].

To address these challenges, we propose a novel FL framework namely Federated Learning based on Adaptive Local Training (FedALT) tailored for wearable-based activity recognition in home health monitoring. Our method employs Autoencoder (AE) equipped local models that combine unsupervised latent representation learning with a Predictor (PD) to classify activities into predefined classes, including both normal daily activities and abnormal actions, such as falls. Specifically, each client's model comprises two components, i.e., an AE and a PD. To enhance the local training process, we introduce the Adaptive Local Training (ALT) algorithm that helps AE learn client-specific latent representations to capture local data patterns (e.g., unique motion signatures from wearables).

The core innovation of FedALT lies in its adaptive mechanism to balance local and global contributions during local model initialization using the ALT algorithm. Our framework, as illustrated in Figure 1, dynamically adjusts the influence of the global AE on each client as follows. When the global AE (i.e., the weights of the encoder (E) and decoder (D) of the global AE in Figure 1) aligns well with a client's local data (e.g., similar motion patterns), the client's AE in $\hat{\phi}_t^k$ learns heavily from the global model $\phi_t^g$, enhancing generalization. When misalignment occurs, the local AE prioritizes its own representations $\phi_{t-1}^k$, while the PD continues to leverage global knowledge to recognize shared classes across clients as in the standard FL technique [9]. The alignment of the global AE is assessed by computing the Reconstruction Error (RE) loss of the global AE on the local data. Importantly, unlike the supervised Cross-Entropy (CE) loss used in prior work such as FedALA [12], the RE loss is an unsupervised loss that does not depend on class labels. This makes the adaptive initialization less sensitive to the heterogeneous distribution of data labels across clients, which is a key advantage for non-IID settings.

We validate our proposed FL framework on three wearable sensor datasets capturing human activities such as falls and daily activities, i.e., MobiAct, MobiFall, and HAR datasets. These datasets inherently exhibit non-IID characteristics due to variations in device orientation, user demographics, and environmental contexts. Each volunteer in these datasets is treated as an individual client in the FL framework, naturally reflecting the data heterogeneity encountered in real-world health monitoring deployments. Our experiments demonstrate that the proposed framework not only improves classification accuracy across all activity types but also achieves particularly strong performance on minority and abnormal action classes, ensuring robustness to data heterogeneity, a critical requirement for real-world deployment in privacy-sensitive applications like elderly care. By enabling adaptive knowledge sharing between local and global models through unsupervised reconstruction-based initialization, our work bridges the gap between personalized learning and collaborative intelligence, advancing FL for scenarios where data diversity and privacy are paramount.

The main contributions of the paper are as follows:

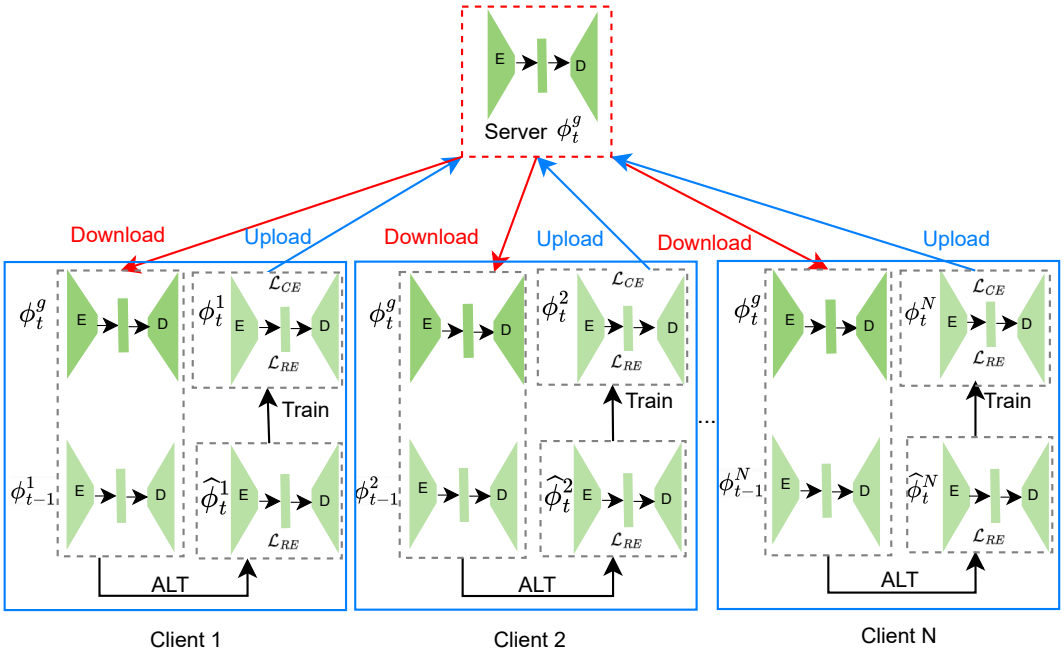



Figure 1. Architecture of proposed system.

- Propose the Adaptive Local Training (ALT) algorithm that uses unsupervised RE loss to initialize weights for the local training process of each client, making the initialization robust to non-IID label distributions across clients.
- Propose the FedALT framework that integrates the ALT algorithm with an AE-based local model architecture for activity classification in home health monitoring, enabling personalized models that adapt to each client's data characteristics.
- Conduct extensive experiments on three human activity datasets (MobiAct, MobiFall, and HAR) to demonstrate the effectiveness of the proposed framework, particularly for classifying abnormal actions such as falls under heterogeneous data distributions.

The rest of the paper is organized as follows. Section 2 highlights recent research for activity recognition and fall detection in FL settings. The proposed framework is then presented in Section 3. This is followed by Section 4 that presents experimental settings. Section 5 discusses the experimental results. Finally, in Section 6, we present some conclusions and suggest future work.

## 2. Related Work

The traditional FL framework known as FedAvg [9] has been widely adopted for training deep learning models using decentralized data. FedAvg has been applied across various domains. For instance, Hard et al. utilized the FedAvg framework for mobile keyboard prediction tasks [13], demonstrating its potential for developing personalized language models on mobile devices through FL. Their research emphasized the benefits of FedAvg in safeguarding user privacy while enhancing prediction accuracy and reducing communication overhead. Additionally, Reddi et al. [14]

introduced an extension of FedAvg called Adaptive Federated Optimization (AFO), which incorporates adaptive learning rates tailored to each client's local data distribution and performance. This modification aims to enhance convergence speed and generalization in FL settings. In another application, Li et al. [15] combined FL with deep autoencoders (AEs) for intrusion detection in IoT networks, proposing a federated deep autoencoder framework where local models are trained on edge devices. Their study showcased the efficacy of FL in identifying intrusions within IoT environments. Similarly, Mothukuri et al. [16] employed the FL framework for anomaly detection, focusing on recognizing intrusions in IoT networks using decentralized on-device data. For secure client weights, Zhen et al. [17] introduced a secure aggregation scheme, an efficient encrypted aggregation scheme designed to thwart gradient inversion attacks in FL, underscoring the critical need for robust privacy-preserving mechanisms within FL systems to prevent sensitive data leakage

However, above FL techniques frequently encounters challenges in statistically heterogeneous settings, such as FL with Non-IID and imbalanced data [10]. Recently, there has been significant attention towards personalization of FL systems as a means to address statistical heterogeneity in FL. Wu et al. [7] proposed the FedHome framework which is a cloud-edge FL framework for in-home health monitoring. FedHome learns a shared global model in the cloud by aggregating data from multiple homes at the network edges while preserving data privacy. To overcome challenges in imbalanced of user's monitoring data, the local model of FedHome refines the model by using the SMOTE algorithm to handle class-balanced dataset derived from the user's personal data, improving accuracy in health monitoring. However, FedHome does not consider clients' Non-IID data distribution in the home health monitoring system.

Recently, personalized aggregation-based FL (pFL) has garnered significant attention for its ability to train on Non-IID client data. Unlike traditional FL, which focuses on developing a single global model, pFL techniques aim to create personalized models tailored to each client's unique data characteristics.

A notable contribution in this area is the Adaptive Personalized Federated Learning (APFL) framework introduced by Deng et al. [18]. This framework features an adaptive aggregation mechanism that dynamically adjusts the weights assigned to both the global model and the personalized model during the aggregation phase of local training. This approach effectively balances the performance of the global model with that of the personalized model. In addition, APFL incorporates a proximal term into the optimization objective, encouraging the personalized model to remain close to the global model. This strategy helps to retain the knowledge acquired from the global model while still allowing individual customization.

Another significant development is FedFomo, proposed by Zhang et al. [19], which emphasizes local model aggregation at each iteration to initialize the local model. This method estimates client-specific weights for aggregation by leveraging local models from other clients. However, a drawback of FedFomo is its requirement to collect models from all clients, not just the global model, leading to increased communication overhead.

More recently, Zhang et al. [12] introduced Adaptive Local Aggregation for Personalized Federated Learning (FedALA), which employs a fine-grained Adaptive Local Aggregation (ALA) approach. The ALA algorithm facilitates element-wise aggregation of the global and local models, allowing each client to align more closely with its specific local objectives during model initialization. Since FedALA primarily modifies the local initialization phase of the FL framework, it can be easily integrated into existing FL

methods to enhance their performance without necessitating changes to other components of the learning process.

In this paper, we propose a novel FL framework namely Personalized Federated Learning based on Adaptive Local Training (FedALT) for IoT anomaly detection system. The proposed system utilizes the local model architecture, which has two components, i.e., the AE and the PD components, to effectively learn the client's data collect from IoT sensors. Moreover, we adapt the ALA algorithm [12] by only using the unsupervised loss, i.e., the RE loss, for client's weight initialization while the ALA algorithm uses the CE loss. The RE loss does not use the label information for calculation like the CE loss. Thus, it helps the initialization weight process of local training more generative.

## 3. Proposed Models

In FL settings, the server aggregates the trained client models or local models to create a global model. However, this global model exhibits subpar generalization performance on each individual client. The reasons for the poor generalization of the global model can vary. It could be due to the inherent heterogeneity among the clients' data distributions, leading to differences in data characteristics, feature representations, or underlying relationships. Additionally, the aggregation process itself may not adequately account for these variations, resulting in a model that fails to capture the unique aspects of each client's data. To address this challenge, we propose a personalized FL technique, i.e., FedALT, that aims to tailor the global model to each individual client's data while still leveraging the collective knowledge from other clients.

In this section, we first present the notations of the proposed FL framework together with the description of local model. Then, we introduce the proposed solution, i.e., FedALT, to personalize client's model at each training round. Then, we present the proposed FL framework, namely FedALT, using the ALT algorithm for the anomaly detection in health monitoring.

### 3.1. Local Model

The local model in each client of FedALT includes two parts, i.e., an AE and a PD module. The AE aims to extract the latent representation $z$ of the original data $x$ and to reconstruct the original data from the latent representation $z$ at the output. The PD attempts to classify the latent representation $z$ into predefined activity classes, including both normal daily activities and abnormal actions such as falls.

The loss function of the local model includes two terms as in Eq. 1.

$$\mathcal{L}_{\text{CAE}} = \alpha \times \mathcal{L}_{\text{RE}} + \beta \times \mathcal{L}_{\text{CE}}, \tag{1}$$

where $\alpha$ and $\beta$ are the trade-off parameters that control the contributions of each term to the total loss function $\mathcal{L}_{\text{CAE}}$. In this work, we set $\alpha = 1$ and $\beta = 1$ for all experiments, meaning both the reconstruction and classification losses contribute equally to the training objective.

The first term in the loss function is the RE loss $\mathcal{L}_{\text{RE}}$. This loss forces the AE to faithfully reconstruct the original data at the output, thereby learning meaningful latent representations. It is calculated as follows.

$$\mathcal{L}_{\text{RE}} = \frac{1}{N}\sum_{i=1}^{N} l\left(x^i, \hat{x}^i\right), \tag{2}$$

where $l\left(x^i, \hat{x}^i\right)$ measures the difference between the input $x^i$ and the reconstructed output $\hat{x}^i$. In the AE-based model, the mean squared error (MSE) is commonly used [20].

The second term is the CE loss $\mathcal{L}_{\text{CE}}$ that guides the PD in the classification task. The cross-entropy loss is calculated as follows.

$$\mathcal{L}_{\text{CE}} = -\frac{1}{N}\sum_{i=1}^{N}\sum_{j=1}^{M} y_j^i \times \log(p_j^i), \tag{3}$$

where $M$ is the number of activity classes and $N$ is the number of training data samples. $y_j^i$ is the ground-truth label indicator of class $j$ for the data sample $x^i$. $p_j^i$ is the Softmax probability output of class $j$ for the input data sample $x^i$.

### 3.2. Adaptive Local Training Algorithm

Our proposed FL system for health monitoring is called FedALT (Figure 1). FedALT includes a server and $K$ clients. Each client $k$ has its own private training dataset $D^k$. The FedALT system introduces the Adaptive Local Training (ALT) algorithm that dynamically learns initial weights of the local model by integrating contributions from both the global model $\phi_t^g$ and the local model of the previous training round $\phi_{t-1}^k$. The ALT algorithm utilizes a subset of local data to adjust the contribution of $\phi_t^g$ and $\phi_{t-1}^k$ to produce the initialized local model $\hat{\phi}_t^k$. Thus, the FedALT system allows the initial weights of the local model to effectively integrate knowledge from the global model while retaining client-specific information. Specifically, let $\phi_{t-1}^{k,\text{AE}}$ be the weights of the AE part in the local model of client $k$, and let $\phi_{t-1}^{k,\text{PD}}$ be the weights of the PD part. In the ALT algorithm, only the AE weights $\phi_{t-1}^{k,\text{AE}}$ are updated, while the PD weights are frozen and directly copied from the global model (Line 9 in Algorithm 2). Different from the previous work FedALA [12], which uses the supervised CE loss to learn the adaptive weights for the entire local model, ALT learns the initial weights for only the AE part using the unsupervised RE loss $\mathcal{L}_{\text{RE}}$. Since the RE loss does not require class labels, it mitigates the bias of the global model, which can arise due to heterogeneous label distributions across clients in non-IID settings, during the local initialization step. Consequently, the initialized AE weights $\hat{\phi}_t^{k,\text{AE}}$ are better equipped to transfer knowledge from other clients, enhancing the model's ability to generalize across varied data distributions.

The ALT algorithm for each client $k$ is presented in Algorithm 2. The algorithm

**Algorithm 1** The Adaptive Local Training (ALT) algorithm.

1: **Input:** $\phi_{t-1}^k$: the local model of client $k$ at round $t-1$; $\phi_t^g$: the global model at round $t$; $\eta$: learning rate; $T_{\text{ALT}}$: maximum number of iterations; $\epsilon$: convergence threshold.
2: **Output:** $\hat{\phi}_t^k$: the initialized local model of client $k$ at round $t$.
3: Initialize the temporary weight $w^{\text{AE}} \leftarrow \mathbf{1} \in \mathbb{R}^d$.
4: Initialize $\hat{\phi}_t^{k,\text{AE}}$ using Eq. 4:
$\hat{\phi}_t^{k,\text{AE}} \leftarrow \phi_{t-1}^{k,\text{AE}} + (\phi_t^{g,\text{AE}} - \phi_{t-1}^{k,\text{AE}}) \odot w^{\text{AE}}$
5: Select a sub-dataset $d$ from $d^k$ by randomly sampling $r\%$.
6: **for** iter = 1 to $T_{\text{ALT}}$ **do**
7: Compute the RE loss $\mathcal{L}_{\text{RE}}$ of $\hat{\phi}_t^{k,\text{AE}}$ on $d^k$ using Eq. 2.
8: Compute the gradient $\delta(\hat{\phi}_t^{k,\text{AE}}) = \nabla_{\hat{\phi}_t^{k,\text{AE}}} \mathcal{L}_{\text{RE}}$.
9: Update $w^{\text{AE}}$ by Eq. 5.
10: Update $\hat{\phi}_t^{k,\text{AE}}$ by Eq. 6.
11: **if** $|\Delta\mathcal{L}_{\text{RE}}| < \epsilon$ **then break**
12: **end for**
13: $\hat{\phi}_t^{k,\text{PD}} \leftarrow \phi_t^{g,\text{PD}}$
14: **Return** $\hat{\phi}_t^k = \{\hat{\phi}_t^{k,\text{AE}}, \hat{\phi}_t^{k,\text{PD}}\}$.

introduces a temporary weight vector $w^{\text{AE}} \in \mathbb{R}^d$, where $d$ is the total number of parameters in the AE. Each element $w_i^{\text{AE}}$ controls how much the $i$-th parameter of the global AE contributes to the local initialization. The weight vector $w^{\text{AE}}$ is initialized with all elements set to 1.

In Line 4 of Algorithm 2, the AE weights of the local model are initialized by blending the previous local AE weights $\phi_{t-1}^{k,\text{AE}}$ with the global AE weights $\phi_t^{g,\text{AE}}$, controlled by the temporary weight vector $w^{\text{AE}}$:

$$\hat{\phi}_t^{k,\text{AE}} = \phi_{t-1}^{k,\text{AE}} + (\phi_t^{g,\text{AE}} - \phi_{t-1}^{k,\text{AE}}) \odot w^{\text{AE}}, \quad (4)$$

where $\odot$ denotes element-wise (Hadamard) multiplication. Since $w^{\text{AE}}$ is initialized as $\mathbf{1}$, the initial value of $\hat{\phi}_t^{k,\text{AE}}$ equals the global AE weights

$\phi_t^{g,\mathrm{AE}}$. The subsequent iterative loop (Lines 6–12) then refines $w^{\mathrm{AE}}$ to selectively blend local and global parameters based on the RE loss computed on the local sub-dataset $d^k$.

At each iteration, the algorithm first computes the RE loss of the current $\hat{\phi}_t^{k,\mathrm{AE}}$ on the sub-dataset $d^k$, then computes the gradient $\delta(\hat{\phi}_t^{k,\mathrm{AE}}) = \nabla_{\hat{\phi}_t^{k,\mathrm{AE}}} \mathcal{L}_{\mathrm{RE}}$ with respect to the AE parameters. This gradient is used to update the temporary weight vector $w^{\mathrm{AE}}$ as follows:

$$w^{\mathrm{AE}} = \sigma\Big(w^{\mathrm{AE}} - \eta \cdot \Big(\delta(\hat{\phi}_t^{k,\mathrm{AE}}) \odot (\phi_t^{g,\mathrm{AE}} - \phi_{t-1}^{k,\mathrm{AE}})\Big),\ 0,\ 1\Big), \tag{5}$$

where $\sigma(\cdot, 0, 1)$ is a clipping function that constrains each element of $w^{\mathrm{AE}}$ to the range $[0, 1]$ as in [12], $\eta$ is the learning rate, and $\odot$ denotes element-wise multiplication. Intuitively, if the gradient direction aligns with the difference between global and local AE parameters for a given parameter $i$, the corresponding weight $w_i^{\mathrm{AE}}$ decreases, reducing the influence of the global model for that parameter. Conversely, if they are misaligned, $w_i^{\mathrm{AE}}$ increases, allowing greater transfer from the global model.

After updating $w^{\mathrm{AE}}$, the AE weights are recomputed using the refined weight vector:

$$\hat{\phi}_t^{k,\mathrm{AE}} = \phi_{t-1}^{k,\mathrm{AE}} + (\phi_t^{g,\mathrm{AE}} - \phi_{t-1}^{k,\mathrm{AE}}) \odot w^{\mathrm{AE}}. \tag{6}$$

The iterative loop terminates when the change in RE loss between consecutive iterations falls below a threshold $\epsilon$, or when the maximum number of iterations $T_{\mathrm{ALT}}$ is reached. This ensures that the algorithm always terminates even if the RE loss is slow to converge. After the loop completes, the PD weights are directly copied from the global model (Line 13), and the full initialized local model $\hat{\phi}_t^k$ is returned for local training.

### 3.3. System Architecture

The proposed FL system named Federated Learning based on Adaptive Local Training (FedALT) is described in Algorithm 3. The system consists of a central server and $K$ clients.

**Algorithm 2** The Adaptive Local Training (ALT) algorithm.

1: **Input:** $\phi_{t-1}^k$: the local model of client $k$ at round $t-1$; $\phi_t^g$: the global model at round $t$; $\eta$: learning rate; $T_{\mathrm{ALT}}$: maximum number of iterations; $\epsilon$: convergence threshold.
2: **Output:** $\hat{\phi}_t^k$: the initialized local model of client $k$ at round $t$.
3: Initialize the temporary weight $w^{\mathrm{AE}} \leftarrow \mathbf{1} \in \mathbb{R}^d$.
4: Initialize $\hat{\phi}_t^{k,\mathrm{AE}}$ using Eq. 4:
$\hat{\phi}_t^{k,\mathrm{AE}} \leftarrow \phi_{t-1}^{k,\mathrm{AE}} + (\phi_t^{g,\mathrm{AE}} - \phi_{t-1}^{k,\mathrm{AE}}) \odot w^{\mathrm{AE}}$
5: Select a sub-dataset $d$ from $d^k$ by randomly sampling $r\%$.
6: **for** iter = 1 to $T_{\mathrm{ALT}}$ **do**
7: Compute the RE loss $\mathcal{L}_{\mathrm{RE}}$ of $\hat{\phi}_t^{k,\mathrm{AE}}$ on $d^k$ using Eq. 2.
8: Compute the gradient $\delta(\hat{\phi}_t^{k,\mathrm{AE}}) = \nabla_{\hat{\phi}_t^{k,\mathrm{AE}}} \mathcal{L}_{\mathrm{RE}}$.
9: Update $w^{\mathrm{AE}}$ by Eq. 5.
10: Update $\hat{\phi}_t^{k,\mathrm{AE}}$ by Eq. 6.
11: **if** $|\Delta \mathcal{L}_{\mathrm{RE}}| < \epsilon$ **then break**
12: **end for**
13: $\hat{\phi}_t^{k,\mathrm{PD}} \leftarrow \phi_t^{g,\mathrm{PD}}$
14: **Return** $\hat{\phi}_t^k = \{\hat{\phi}_t^{k,\mathrm{AE}}, \hat{\phi}_t^{k,\mathrm{PD}}\}$.

It begins by initializing a global model $\phi_0^g$ on the server, which is then broadcast to all $K$ clients. In each communication round $t$, each client $k$ first initializes its local model $\hat{\phi}_t^k$ using the ALT algorithm (Algorithm 2), which adaptively blends the global model $\phi_t^g$ with the previous local model $\phi_{t-1}^k$ as described in Section 3.2. The client then trains the initialized local model $\hat{\phi}_t^k$ on its private training data by minimizing the loss function in Eq. 1 for $p$ local epochs, producing the updated local model $\phi_t^k$.

Each client sends its trained model $\phi_t^k$ to the server for weighted averaging:

$$\phi_{t+1}^g = \sum_{k=1}^{K} \frac{|D^k|}{\sum_{j=1}^{K} |D^j|} \phi_t^k, \tag{7}$$

**Algorithm 3** Federated Learning based on Adaptive Local Training (FedALT)

**Input:** Initial global model $\phi_0^g$; set of $K$ clients with private training data $\{D^1, D^2, \ldots, D^K\}$; number of communication rounds $T$; number of local epochs $p$.
**Output:** Personalized local models $\{\phi_T^1, \phi_T^2, \ldots, \phi_T^K\}$.
Initialize weights for the global model $\phi_0^g$.
Broadcast the global model $\phi_0^g$ to all $K$ clients.
**for** $t = 1$ **to** $T$ **do**
  **for** each client $k \in \{1, 2, \ldots, K\}$ **do**
    Initialize the local model $\hat{\phi}_t^k$ using the **ALT algorithm** (Algorithm 2).
    Train local model $\hat{\phi}_t^k$ on $D^k$ by minimizing $\mathcal{L}_{\text{CAE}}$ in Eq. 1 for $p$ local epochs to obtain $\phi_t^k$.
    Send $\phi_t^k$ to the server.
  **end for**
  **Server aggregation:** $\phi_{t+1}^g \leftarrow \sum_{k=1}^{K} \frac{|D^k|}{\sum_{j=1}^{K} |D^j|} \phi_t^k$ (Eq. 7)
  Broadcast $\phi_{t+1}^g$ to all $K$ clients.
**end for**

where $|D^k|$ is the number of training samples of client $k$. This aggregation weights each client's contribution proportionally to its dataset size, following the standard FedAvg strategy [9]. The updated global model $\phi_{t+1}^g$ is then broadcast to all clients for the next round. This process is repeated for $T$ communication rounds, iteratively improving both the global model and the personalized local models while keeping the training data decentralized on the clients' devices.

## 4. Experimental Settings

This section provides a comprehensive description of the datasets utilized in our experiments, along with the specific configuration of experimental parameters. In addition, it presents the performance metrics that were employed to evaluate the effectiveness of the proposed FedALT framework presented in this paper.

### *4.1. Datasets*

We evaluate our proposed model on three public Human Activity Recognition (HAR) datasets, including MobiAct [21], MobiFall [22] and HAR [23]. These datasets consist of data collected from various types of wearable devices, capturing both daily living activities and fall events.

The **MobiAct** dataset was generated by 67 volunteers, including 51 males and 16 females. Each volunteer wears a Samsung Galaxy S3 device equipped with the LSM330DLC inertial sensor comprising a 3D accelerometer and gyroscope. The recorded activities are annotated into one of 15 activity classes. These classes encompass three category groups, i.e., activities of daily living (ADL), activities resembling falls (Fall-like), and actual falls. The details about this dataset are presented in Table 1.

The **MobiFall** dataset follows a similar recording scenario to the MobiAct dataset and consists of 13 activity classes. A total of 24 volunteers, consisting of 17 males and 7 females, participated in the data collection. The recorded activities have been categorized into three categories as in Table 2.

The **HAR** dataset was created by 30 participants aged 19 to 48 [23]. The volunteers wear a Samsung Galaxy S II and perform six preset activities, i.e., walking, walking upstairs, walking downstairs, sitting, standing, and lying. A detailed description of the activity classes in the HAR dataset is provided in Table 3.

Table 1. Description of the MobiAct dataset. The "No. Samples" column reports the number of raw activity recordings before the sliding-window preprocessing

| Category | Code | Activity | Description | No. Samples |
|---|---|---|---|---|
| ADLs | STD | Standing | Standing with subtle movements | 32681 |
| | WAL | Walking | Normal walking | 42969 |
| | JOG | Jogging | Jogging | 3988 |
| | JUM | Jumping | Continuous jumping | 3906 |
| | STU | Stairs up | Stairs up (10 stairs) | 983 |
| | STN | Stairs down | Stairs down (10 stairs) | 991 |
| | SIT | Sitting on chair | Sitting on a chair with subtle movements | 1857 |
| | CHU | Sit to stand | Transition from sitting to standing | 115 |
| Fall -like | CSI | Car step in | Step in a car | 416 |
| | CSO | Car step out | Step out a car | 426 |
| | SCH | Stand to sit | Transition from standing to sitting | 365 |
| Falls | FOL | Forward lying | Fall forward from standing, use of hands to dampen fall | 920 |
| | FKL | Front knees lying | Fall forward from standing, first impact on knees | 934 |
| | BSC | Back sitting chair | Fall backward while trying to sit on a chair | 921 |
| | SDL | Sideward lying | Fall sidewards from standing, bending legs | 918 |

Table 2. Description of the MobiFall dataset. The "No. Samples" column reports the number of raw activity recordings before the sliding-window preprocessing

| Category | Code | Activity | Description | No. Samples |
|---|---|---|---|---|
| ADLs | STD | Standing | Standing with subtle movements | 6150 |
| | WAL | Walking | Normal walking | 6083 |
| | JOG | Jogging | Jogging | 567 |
| | JUM | Jumping | Continuous jumping | 559 |
| | STU | Stairs up | Stairs up (10 stairs) | 147 |
| | STN | Stairs down | Stairs down (10 stairs) | 152 |
| Fall -like | CSI | Car-step in | Step in a car | 67 |
| | CSO | Car-step out | Step out a car | 74 |
| | SCH | Stand to sit | Transition from standing to sitting | 67 |
| Falls | FOL | Forward-lying | Fall forward from standing, use of hands to dampen fall | 388 |
| | FKL | Front-knees-lying | Fall forward from standing, first impact on knees | 407 |
| | BSC | Back-sitting-chair | Fall backward while trying to sit on a chair | 404 |
| | SDL | Sideward-lying | Fall sidewards from standing, bending legs | 387 |

The raw sensor recordings in these datasets are preprocessed into fixed-size data samples using a sliding-window approach based on the Cartesian coordinate system [24]. Each data sample is a matrix with the shape $6 \times 200$ for the MobiAct and MobiFall datasets, or the shape $9 \times 128$ for the HAR dataset [7]. Note that the sample counts reported in Tables 1, 2, and 3 represent the number of raw activity recordings, while Table 4 reports the total number of sliding-window samples used for training and evaluation. The sliding-window preprocessing generates multiple overlapping samples from each raw recording,

which explains the difference between the two counts (e.g., 92,390 raw recordings versus 923,790 sliding-window samples for MobiAct).

Table 3. Activity classes in the HAR dataset

| Code | Activity | No. samples |
|---|---|---|
| WALKING | Walking | 1722 |
| WALKING _UPSTAIR | Walking upstairs | 1544 |
| WALKING _DOWNSTAIR | Walking downstairs | 1406 |
| SITTING | Sitting | 1777 |
| STANDING | Standing | 1906 |
| LAYING | Laying | 1944 |

### 4.2. Parameter Settings

In this study, each volunteer in the datasets is considered as a client in the FL framework. The datasets are randomly divided into a 75% training set and a 25% testing set for all clients. The statistical information of the datasets used in our experiments is provided in Table 4.

Table 4. Statistics for the MobiAct, MobiFall, and HAR datasets. The "No. samples" column reports the number of sliding-window samples used for training and evaluation

| Dataset | No. clients | No. classes | No. samples |
|---|---|---|---|
| MobiAct | 67 | 15 | 923,790 |
| MobiFall | 24 | 13 | 15,452 |
| HAR | 30 | 6 | 10,299 |

To evaluate the effectiveness of the proposed solution, we compare FedALT against various FL frameworks: FedAvg [9], FedFomo [19], APFL [18], FedHome [7], and FedALA [12]. Among these baselines, FedHome and FedALT use the AE-based local model architecture (i.e., AE + PD), while FedAvg, FedFomo, APFL, and FedALA use CNN-based local models. The reason for this design is as follows. The ALT algorithm in FedALT requires an AE component to compute the unsupervised RE loss for adaptive weight initialization; thus, the AE-based architecture is integral to our method rather than an arbitrary choice. To isolate the effect of the AE-based architecture from the effect of the ALT mechanism, we include FedHome as a baseline that also uses the AE-based local model but applies the standard FedAvg aggregation strategy without adaptive local initialization. Therefore, comparing FedALT against FedHome directly demonstrates the contribution of the ALT algorithm, while comparing FedHome against FedAvg reveals the impact of the AE-based architecture. The CNN-based baselines (FedAvg, FedFomo, APFL, FedALA) are included to provide a comprehensive comparison against widely adopted FL frameworks in the literature.

For the ALT algorithm, we set the sub-dataset sampling ratio $r = 20\%$, the maximum number of ALT iterations $T_{\text{ALT}} = 50$, the convergence threshold $\epsilon = 10^{-4}$, and the ALT learning rate $\eta = 0.01$.

The FL systems are trained with consistent hyper-parameters across the HAR, MobiFall, and MobiAct datasets as follows. The activation function used throughout all FL training is ReLU. Stochastic Gradient Descent (SGD) is employed as the local optimizer with a learning rate of 0.01. Training is conducted over $p = 5$ local epochs per global round, with a total of $T = 50$ global communication rounds.

### 4.3. Evaluation Metrics

We evaluate the performance of the proposed FL solution using three metrics, i.e., Precision, Recall, and F1 score. Let $C$ define the number of classes in a dataset. These metrics are described as follows.

- The Precision score for a given class $j$ ($j = 1, 2, \ldots, C$), i.e., $\text{P}_j$, is calculated by the following equation.

$$\text{P}_j = \text{TP}_j/(\text{TP}_j + \text{FP}_j), \tag{8}$$

where $TP_j$ is the number of samples correctly predicted as class $j$, and $FP_j$ is the number of samples that do not belong to class $j$ but are incorrectly predicted as class $j$.

- The Recall score for a given class $j$ ($j = 1, 2, \ldots, C$), i.e., $R_j$ measures the proportion of correctly predicted samples for class $j$ among all actual samples of class $j$:

$$R_j = TP_j/(TP_j + FN_j), \quad (9)$$

where $FN_j$ is the number of samples that belong to class $j$ but are incorrectly predicted as other classes.

- The F1 score for a given class $j$ ($j = 1, 2, \ldots, C$), i.e., $F1_j$, combines Precision and Recall to provide a balanced evaluation:

$$F1_j = 2 \times (P_j \times R_j)/(P_j + R_j), \quad (10)$$

where $P_j$ and $R_j$ are the Precision and Recall for the class $j$ obtained from Eq. (8) and Eq. (9), respectively.

To assess overall performance, we compute the Macro-Average of Precision, Recall, and F1 scores across all classes:

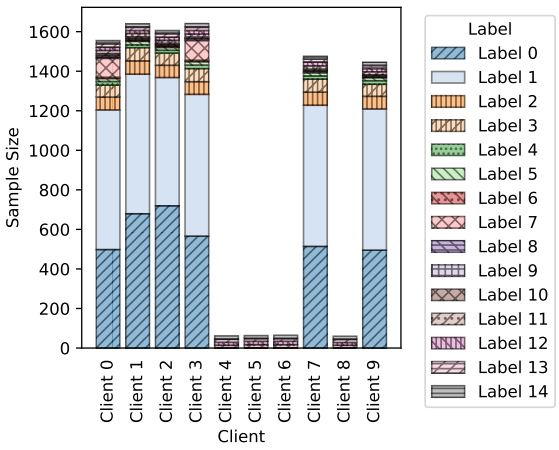
$$\text{Macro-Average} = 1/C \sum_{j=1}^{C} M_j, \quad (11)$$

where $M_j$ is a metric, e.g., Precision, Recall, F1 scores, for the class $j$. This metric is particularly effective for assessing classifiers on highly imbalanced datasets, making it the primary performance indicator for evaluating FL systems in this study.

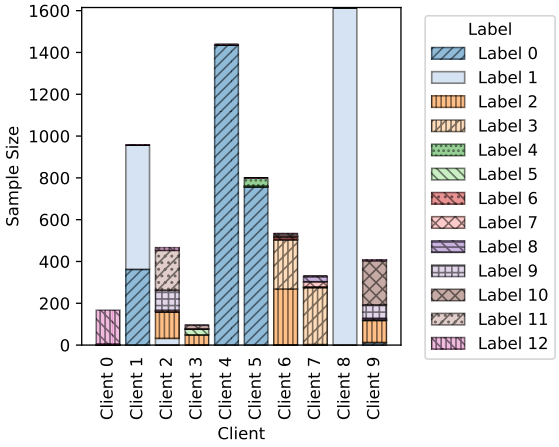
## 5. Results and Analysis

### 5.1. Activity Classification Results

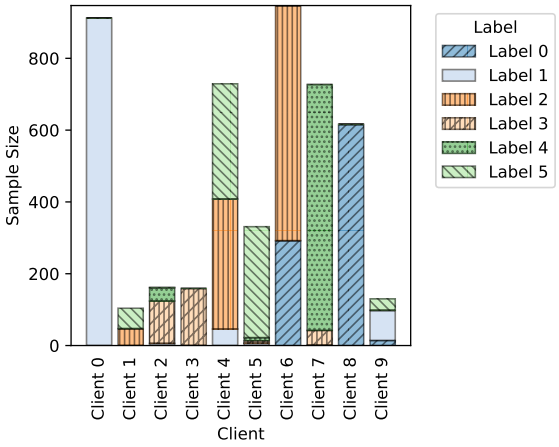
This section compares the macro average Precision (P), Recall (R), and F1 scores of the




(a) MobiAct dataset




(b) MobiFall dataset




(c) HAR dataset

Figure 2. Visualization of data distribution in clients.

various FL systems. Table 5 presents the macro average P, R, F1 scores across all classes in the testing datasets.

As shown in Table 5, most FL frameworks improve accuracy compared to FedAvg on the HAR dataset. This is expected because the HAR dataset has only six activity classes with a relatively balanced distribution across clients, resulting in a less severe non-IID setting compared with the other datasets. On the highly non-IID datasets, i.e., MobiFall and MobiAct, the non-personalized or weakly personalized methods (FedAvg, APFL, and FedHome) perform poorly. In contrast, the personalized FL frameworks (FedFomo, FedALA, and FedALT) achieve substantially better accuracy on these two datasets. Among all methods, FedALT achieves the best or comparable accuracy across almost all metrics and datasets.

To fairly assess the contribution of the proposed ALT mechanism, we highlight two key comparisons. First, comparing FedALT against FedHome is particularly informative because both methods use the same AE-based local model architecture (AE + PD). The only difference is that FedALT applies the ALT algorithm for adaptive local initialization, while FedHome uses the standard FedAvg aggregation without adaptive initialization. On the MobiFall dataset, FedALT achieves an F1 score of 0.86 compared to 0.51 for FedHome, representing a substantial improvement of 0.35. On MobiAct, FedALT improves over FedHome by 0.25 in F1 score (0.75 vs. 0.50). These improvements can be directly attributed to the ALT mechanism, since the backbone architecture is identical. Second, comparing FedALT against FedALA isolates the effect of using unsupervised RE loss versus supervised CE loss for adaptive weight initialization, as both methods employ adaptive local aggregation but differ in the loss function and the scope of adaptation. FedALT outperforms FedALA on MobiFall (F1: 0.86 vs. 0.80), confirming that using RE loss for initializing only the AE weights is more effective than using CE loss for the entire model under non-IID conditions.

Table 5. Macro average of Precision, Recall, and F1-score of activities on the MobiFall, MobiAct, and HAR datasets

| **Dataset** | **MobiFall** | | | **MobiAct** | | | **HAR** | | |
|---|---|---|---|---|---|---|---|---|---|
| **Metric** | **P** | **R** | **F1** | **P** | **R** | **F1** | **P** | **R** | **F1** |
| FedAvg | 0.50 | 0.49 | 0.49 | 0.48 | 0.55 | 0.49 | 0.88 | 0.88 | 0.88 |
| FedFomo | 0.71 | 0.65 | 0.67 | **0.77** | 0.74 | 0.75 | 0.91 | 0.91 | 0.91 |
| APFL | 0.48 | 0.49 | 0.47 | 0.50 | 0.55 | 0.50 | 0.88 | 0.88 | 0.88 |
| FedHome | 0.52 | 0.51 | 0.51 | 0.49 | 0.56 | 0.50 | 0.88 | 0.88 | 0.88 |
| FedALA | 0.82 | 0.78 | 0.80 | **0.77** | 0.74 | 0.75 | **0.97** | **0.97** | **0.97** |
| FedALT | **0.88** | **0.85** | **0.86** | **0.77** | **0.75** | **0.75** | **0.97** | **0.97** | **0.97** |

To further analyze the per-class performance, Table 6 presents the Precision and Recall for each activity class on the MobiFall dataset. Abnormal actions (Fall-like and Falls categories) have significantly fewer data samples compared to normal daily activities (ADLs). For the majority ADL classes (e.g., STD, WAL), all methods perform reasonably well. However, for minority classes with fewer samples, FedAvg and FedHome struggle considerably. Since FedHome uses the same AE-based architecture as FedALT but without adaptive initialization, its poor performance on minority classes confirms that the AE architecture alone is insufficient, while the ALT mechanism is essential for handling class imbalance under non-IID conditions.

Both FedALA and FedALT substantially improve over their respective baselines (FedAvg and FedHome). Notably, FedALT achieves the best accuracy for almost all activity classes. For the Fall actions (e.g., FOL, FKL, BSC, SDL), FedALT achieves Precision and Recall values above 0.83, while other methods fail to reach these scores consistently. This demonstrates that the ALT algorithm, which uses only the unsupervised RE loss for adaptive weight initialization, is more effective than the ALA approach with supervised CE loss,

Table 6. Precision and Recall of each activity class on the MobiFall dataset

| **Algorithm** | | | **FedAVG** | | **FedALA** | | **FedHome** | | **FedALT** | |
|---|---|---|---|---|---|---|---|---|---|---|
| Cate gory | **Action** | **No. Samples** | P | R | P | R | P | R | P | R |
| ADLs | STD | 1567 | 0.98 | 0.99 | **1.00** | **1.00** | 0.98 | 0.99 | **1.00** | **1.00** |
| | WAL | 1507 | 0.97 | 0.97 | 0.98 | **1.00** | 0.97 | 0.97 | **0.99** | **1.00** |
| | JOG | 132 | 0.89 | 0.92 | **0.98** | **0.99** | 0.92 | 0.96 | **0.98** | **0.99** |
| | JUM | 126 | 0.91 | 0.91 | 0.93 | **0.99** | 0.90 | 0.93 | **0.99** | **0.99** |
| | STU | 47 | 0.43 | 0.34 | 0.52 | 0.55 | 0.39 | 0.28 | **0.77** | **0.65** |
| | STN | 44 | 0.30 | 0.23 | 0.64 | **0.91** | 0.44 | 0.27 | **0.75** | 0.62 |
| Fall -like | SCH | 12 | 0.11 | 0.25 | 0.40 | 0.40 | 0.15 | 0.25 | **0.95** | **1.00** |
| | CSI | 16 | 0.19 | 0.31 | 0.43 | 0.46 | 0.27 | 0.38 | **0.50** | **0.62** |
| | CSO | 14 | 0.06 | 0.14 | **0.86** | 0.60 | 0.09 | 0.21 | 0.75 | 0.60 |
| Falls | FOL | 98 | 0.40 | 0.33 | 0.78 | 0.74 | 0.43 | 0.36 | **0.83** | **0.89** |
| | FKL | 83 | 0.41 | 0.30 | 0.87 | 0.78 | 0.39 | 0.37 | **0.94** | **0.89** |
| | BSC | 103 | 0.51 | 0.34 | 0.83 | 0.91 | 0.56 | 0.35 | **1.00** | **0.92** |
| | SDL | 86 | 0.34 | 0.38 | 0.93 | 0.84 | 0.29 | 0.35 | **0.96** | **0.93** |

particularly for minority classes where label-dependent initialization can introduce bias under non-IID distributions.

To explain the varying performance of the FL systems across the three datasets, we visualize the data distribution at the clients in Figure 2 (a), Figure 2 (b), and Figure 2 (c). The data distributions of MobiAct (Figure 2 (a)) and MobiFall (Figure 2 (b)) are highly skewed. Specifically, the sample counts of some classes (e.g., classes 0 and 1 in Figure 2 (a)) are much greater than those of other classes (e.g., classes 13 and 14 in Figure 2 (a)). Moreover, the total number of samples varies substantially across clients (e.g., clients 0, 1, 2, 3, 7, and 9 have much more data than clients 4, 5, 6, and 8 in Figure 2 (a)). In contrast, the HAR dataset exhibits a relatively balanced distribution across both classes and clients. This confirms that MobiFall and MobiAct are highly non-IID datasets, while HAR has a milder non-IID characteristic.

Consequently, methods not specifically designed for personalization, such as FedAvg, perform poorly on MobiFall and MobiAct. Although APFL and FedHome are designed for personalization, they also perform ineffectively on these two datasets. APFL focuses on adjusting the global-to-local model ratio but does not address the class imbalance and severe non-IID problems present in these datasets. FedHome addresses the class imbalance problem within each client through data augmentation but does not specifically handle the non-IID distribution across clients. In contrast, FedALT uses the unsupervised RE loss in its ALT algorithm to adaptively initialize the AE weights, which is inherently less sensitive to label distribution heterogeneity across clients, leading to superior performance on the highly non-IID MobiFall and MobiAct datasets.

### *5.2. Abnormal Activity Evaluation*

This subsection evaluates the effectiveness of FL techniques in classifying abnormal activities.

We group the activities into three categories: activities of daily living (ADLs), fall-like activities (Fall-like), and actual fall activities (Falls)[1].

Table 7. Macro average of Precision, Recall, and F1-score of three activity groups on the MobiFall and MobiAct datasets

| **Dataset** | **MobiFall** | | | **MobiAct** | | |
|---|---|---|---|---|---|---|
| **Metric** | **P** | **R** | **F1** | **P** | **R** | **F1** |
| FedAvg | 0.76 | 0.73 | 0.74 | 0.61 | 0.76 | 0.66 |
| FedFomo | 0.94 | 0.91 | 0.93 | 0.94 | 0.87 | 0.90 |
| APFL | 0.76 | 0.75 | 0.75 | 0.61 | 0.76 | 0.66 |
| FedHome | 0.75 | 0.75 | 0.75 | 0.64 | 0.77 | 0.69 |
| FedALA | **0.96** | 0.90 | 0.93 | 0.93 | 0.84 | 0.88 |
| FedALT | 0.95 | **0.95** | **0.95** | **0.96** | **0.91** | **0.93** |

The macro average results in Table 7 demonstrate the superior performance of the proposed FedALT framework compared to the other FL approaches. FedALT achieves the highest macro average F1-score on both datasets: 0.95 on MobiFall and 0.93 on MobiAct. These results confirm that FedALT can learn robust models that effectively classify activities across the three groups, even when the data is highly heterogeneous across clients.

An important observation is the balance between Precision and Recall achieved by FedALT. On the MobiFall dataset, FedALT achieves a Precision and Recall of 0.95 and 0.95, respectively, indicating a tight alignment between the predicted and true activity groups. In contrast, other methods exhibit a larger gap between Precision and Recall. For example, FedALA achieves a high Precision of 0.96 but a lower Recall of 0.90, suggesting that while it is precise in its predictions, it misses a notable proportion of actual abnormal activities. Similarly, on MobiAct, FedALT maintains a smaller Precision-Recall gap (0.96 vs. 0.91) compared to FedALA (0.93 vs. 0.84). A smaller gap indicates a more balanced model that can accurately identify abnormal activities without sacrificing sensitivity, which is critical for health monitoring applications where missing a fall event (low Recall) can have serious consequences.

To further isolate the contribution of the ALT mechanism, we again highlight the comparison between FedALT and FedHome, which share the same AE-based architecture. On MobiFall, FedALT achieves an F1-score of 0.95 compared to 0.75 for FedHome, an improvement of 0.20. On MobiAct, the improvement is 0.24 (0.93 vs. 0.69). Since the only difference between these two methods is the ALT algorithm, this improvement is entirely attributable to the adaptive local initialization using RE loss.

Table 8 presents the per-group Precision and Recall on the MobiAct dataset. For ADL activities, FedAvg, FedALA, and FedALT all achieve perfect or near-perfect scores, indicating that classifying majority activities is straightforward for most methods. FedHome achieves slightly lower but still strong results with Precision of 0.99 and Recall of 0.97.

The differences become more pronounced for the minority activity groups. For Fall-like activities, FedALT achieves the highest Precision of 0.90 and Recall of 0.77, substantially outperforming FedAvg (P: 0.33, R: 0.49) and FedHome (P: 0.39, R: 0.46). The comparison between FedALT and FedHome on this challenging category is particularly revealing: both use the AE-based architecture, yet FedALT's Precision is more than double that of FedHome (0.90 vs. 0.39), demonstrating the significant impact of the ALT mechanism on minority class classification.

For actual Falls, FedALT achieves the best Precision of 0.98 and matches FedALA with a Recall of 0.96. FedAvg and FedHome have notably lower Precision for fall detection (0.49

[1]We conduct these experiments on the MobiFall and MobiAct datasets because these datasets contain defined fall activities (abnormal activities).

Table 8. Precision and Recall of each activity group on the MobiAct dataset

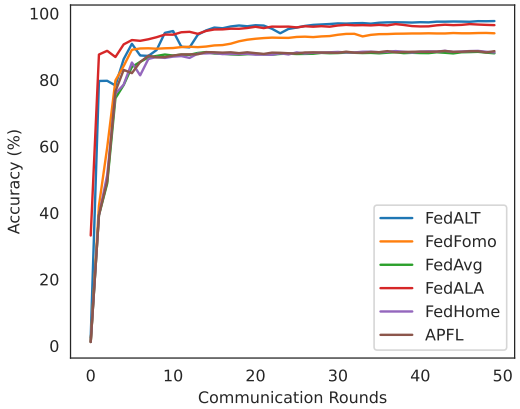
| **Algorithms:** | | **FedAvg** | | **FedALA** | | **FedHome** | | **FedALT** | |
|---|---|---|---|---|---|---|---|---|---|
| **Activities** | **No. Samples** | P | R | P | R | P | R | P | R |
| ADLs | 21788 | **1.00** | 0.96 | **1.00** | **1.00** | 0.99 | 0.97 | **1.00** | **1.00** |
| Fall-like | 329 | 0.33 | 0.49 | 0.85 | 0.57 | 0.39 | 0.46 | **0.90** | **0.77** |
| Falls | 863 | 0.49 | 0.83 | 0.94 | **0.96** | 0.54 | 0.87 | **0.98** | **0.96** |

and 0.54, respectively), indicating high false positive rates. These results confirm that the adaptive local initialization in FedALT, driven by unsupervised RE loss, enables more accurate and balanced classification of abnormal activities, which is essential for reliable fall detection in IoT-based health monitoring applications.

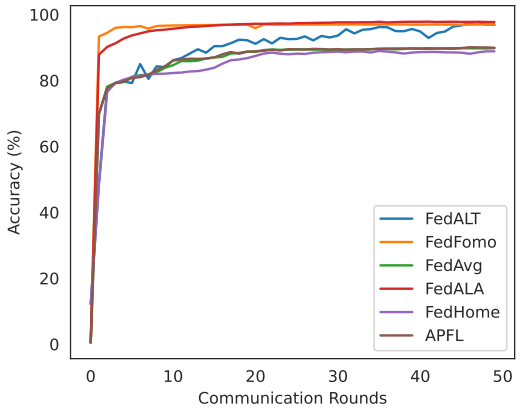
### *5.3. Training Convergence Analysis*

Figure 3 shows the training accuracy of the evaluated FL techniques on the (a) MobiFall and (b) MobiAct datasets over 50 communication rounds. FedALT consistently achieves the highest training accuracy among all methods across both datasets. The superior performance of FedALT can be attributed to the ALT mechanism, which adaptively initializes the AE weights at each round using unsupervised RE loss, enabling the local models to better handle data heterogeneity and device/user differences compared to the other FL methods.

Beyond the final accuracy, the convergence behavior of the different methods provides additional insight. FedALT exhibits a steep positive slope in training accuracy, indicating rapid and sustained improvement across communication rounds. This suggests that the adaptive initialization provided by ALT enables the local models to effectively leverage the global model at each round, leading to faster convergence. In contrast, FedAvg, FedHome, and APFL show relatively flat accuracy curves from the early rounds, indicating that these methods struggle to improve beyond their initial




(a) MobiFall dataset




(b) MobiAct dataset

Figure 3. Training accuracy of FL techniques over communication rounds.

performance on the highly non-IID MobiFall and MobiAct datasets. FedFomo and FedALA show moderate improvement but converge more slowly and to lower accuracy compared to FedALT.

Notably, the comparison between FedALT and FedHome is again instructive, as both share the same AE-based architecture. FedHome's flat convergence curve confirms that the AE architecture alone does not address the non-IID challenge; it is the ALT algorithm that enables the rapid and effective convergence observed in FedALT.

## 6. Conclusion

In this paper, we proposed a novel Federated Learning (FL) framework namely Federated Learning based on Adaptive Local Training (FedALT) for activity classification in home health monitoring systems. The FedALT framework employs a local model consisting of two components, i.e., an Autoencoder (AE) trained in an unsupervised manner to capture latent representations of sensor data, and a Predictor (PD) trained in a supervised manner to classify activities into predefined classes, including both normal daily activities and abnormal actions such as falls. To personalize the local models, we proposed the Adaptive Local Training (ALT) algorithm, which dynamically adjusts the contribution of the global and local AE models during the local initialization step. The ALT algorithm uses only the unsupervised RE loss to learn element-wise adaptive weights that control how much each parameter of the global AE contributes to the local initialization. This design makes the initialization robust to heterogeneous label distributions across clients, which is a key advantage over prior methods such as FedALA that rely on supervised loss for adaptive aggregation. Through extensive evaluations on three wearable sensor datasets (MobiAct, MobiFall, and HAR), we demonstrated that FedALT consistently outperforms existing FL techniques, including FedAvg, FedFomo, APFL, FedHome, and FedALA. In particular, the comparison between FedALT and FedHome, which share the same AE-based architecture, confirms that the performance improvement is directly attributable to the ALT mechanism rather than the model architecture. FedALT achieves particularly strong results in classifying minority and abnormal activity classes such as falls, which is critical for reliable health monitoring applications.

This study can be extended in several directions. First, examining the security concerns associated with FL techniques is crucial for real-world deployment. FedALT shares the AE component between clients and the server during aggregation, and sharing the raw model parameters poses a risk of information leakage [25]. Integrating privacy-preserving mechanisms such as secure aggregation or differential privacy into the FedALT framework would be an important direction for future work. Second, evaluating FedALT on a broader range of IoT-based health monitoring tasks beyond activity recognition, such as vital sign monitoring or sleep quality assessment, would further validate the generalizability of the proposed approach.

## Acknowledgment

This work was supported by the Vingroup Innovation Foundation (VINIF) under Project VINIF.2023.DA059.

## References

[1] S. Y. Y. Tun, S. Madanian, F. Mirza, Internet of Things (IoT) Applications for Elderly Care: A Reflective Review, Aging Clinical and Experimental Research, Vol. 33, 2021, pp. 855–867. https://doi.org/10.1007/s40520-020-01545-9

[2] A. Godinho, F. Cardoso, P. J. Coelho, I. M. Pires, Internet of Things-Based Care Monitoring for The Elderly and Those with Special Needs, Procedia

Computer Science, Vol. 224, 2023, pp. 572–579. https://doi.org/10.1016/j.procs.2023.09.083

[3] S. Mittal, M. Ghosh, A Novel Two-Level Secure Access Control Approach for Blockchain Platform in Healthcare, Int. J. Inf. Secur., Vol. 22, No. 4, 2023, pp. 799–817. https://doi.org/10.1007/s10207-023-00664-4

[4] L. Yi, G. Wang, X. Wang, X. Liu, QSFL: Two-Level Communication-Efficient Federated Learning on Mobile Edge Devices, IEEE Transactions on Services Computing, Vol. 17, No. 6, 2024, pp. 4166–4182. https://doi.org/10.1109/TSC.2024.3455098

[5] J. Kaur, A. Agrawal, R. A. Khan, P2ADF: A Privacy-Preserving Attack Detection Framework in Fog-IoT Environment, Int. J. Inf. Secur., Vol. 22, No. 4, 2023, pp. 749–762. https://doi.org/10.1007/s10207-023-00661-7

[6] R. Al-ani, T. Baker, B. Zhou, Q. Shi, Privacy and Safety Improvement of VANET Data Via A Safety-Related Privacy Scheme, Int. J. Inf. Secur., Vol. 22, No. 4, 2023, pp. 763–783. https://doi.org/10.1007/s10207-023-00662-6

[7] Q. Wu, X. Chen, Z. Zhou, J. Zhang, Fedhome: Cloud-Edge Based Personalized Federated Learning for In-Home Health Monitoring, IEEE Transactions on Mobile Computing, Vol. 21, No. 8, 2020, pp. 2818–2832. https://doi.org/10.48550/arXiv.2012.07450

[8] Y. Xu, Y. Zhu, Z. Wang, H. Xu, Y. Liao, Enhancing Federated Learning Through Layer-Wise Aggregation Over Non-IID Data, IEEE Transactions on Services Computing 2025, pp. 1–14. https://doi.org/10.1109/TSC.2025.3536309

[9] B. McMahan, E. Moore, D. Ramage, S. Hampson, B. A. y Arcas, Communication-Efficient Learning of Deep Networks from Decentralized Data, in: Artificial Intelligence and Statistics, 2017, pp. 1273–1282. https://doi.org/10.48550/arXiv.1602.05629

[10] P. Kairouz, H. B. McMahan, B. Avent, A. Bellet, M. Bennis, A. N. Bhagoji, K. Bonawitz, Z. Charles, G. Cormode, R. Cummings, et al., Advances and Open Problems in Federated Learning, Foundations and Trends® in machine learning, Vol. 14, No. 1–2, 2021, pp. 1–210. https://doi.org/10.48550/arXiv.1912.04977

[11] K. Ren, G. Liao, Q. Ma, X. Chen, Differentially Private Auction Design for Federated Learning With Non-IID Data, IEEE Transactions on Services Computing, Vol. 17, No. 5, 2024, pp. 2236–2247. https://doi.org/10.1109/TSC.2023.3332102

[12] J. Zhang, Y. Hua, H. Wang, T. Song, Z. Xue, R. Ma, H. Guan, Fedala: Adaptive Local Aggregation for Personalized Federated Learning, in: Proceedings of the AAAI Conference on Artificial Intelligence, Vol. 37, 2023, pp. 11237–11244. https://doi.org/10.48550/arXiv.2212.01197

[13] A. Hard, K. Rao, R. Mathews, S. Ramaswamy, F. Beaufays, S. Augenstein, H. Eichner, C. Kiddon, D. Ramage, Federated Learning for Mobile Keyboard Prediction, ArXiv Preprint ArXiv:1811.03604 (2018). https://doi.org/10.48550/arXiv.1811.03604

[14] S. Reddi, Z. Charles, M. Zaheer, Z. Garrett, K. Rush, J. Konečnỳ, S. Kumar, H. B. McMahan, Adaptive Federated Optimization, ArXiv Preprint ArXiv:2003.00295 (2020). https://doi.org/10.48550/arXiv.2003.00295

[15] B. Li, Y. Wu, J. Song, R. Lu, T. Li, L. Zhao, DeepFed: Federated Deep Learning for Intrusion Detection in Industrial Cyber-Physical Systems, IEEE Transactions on Industrial Informatics, Vol. 17, No. 8, 2021, pp. 5615–5624. https://doi.org/10.1109/TII.2020.3023430

[16] V. Mothukuri, P. Khare, R. M. Parizi, S. Pouriyeh, A. Dehghantanha, G. Srivastava, Federated-Learning-Based Anomaly Detection for IoT Security Attacks, IEEE Internet of Things Journal, Vol. 9, No. 4, 2022, pp. 2545–2554. https://doi.org/10.1109/JIOT.2021.3077803

[17] Z. Yang, S. Yang, Y. Huang, J.-F. Martínez, L. López, Y. Chen, AAIA: An Efficient Aggregation Scheme Against Inverting Attack for Federated Learning, Int. J. Inf. Secur., Vol. 22, No. 4, 2023, pp. 919–930. https://doi.org/10.1007/s10207-023-00670-6

[18] Y. Deng, M. M. Kamani, M. Mahdavi, Adaptive Personalized Federated Learning, ArXiv Preprint ArXiv:2003.13461 (2020). https://doi.org/10.48550/arXiv.2003.13461

[19] M. Zhang, K. Sapra, S. Fidler, S. Yeung, J. M. Alvarez, Personalized Federated Learning with First Order Model Optimization, ArXiv Preprint ArXiv:2012.08565 (2020). https://doi.org/10.48550/arXiv.2012.08565

[20] L. Vu, V. L. Cao, Q. U. Nguyen, D. N. Nguyen, D. T. Hoang, E. Dutkiewicz, Learning Latent Representation for IoT Anomaly Detection, IEEE Transactions on Cybernetics, Vol. 52, No. 5, 2022, pp. 3769–3782. https://doi.org/10.1109/TCYB.2020.3013416

[21] G. Vavoulas, C. Chatzaki, T. Malliotakis, M. Pediaditis, M. Tsiknakis, The Mobiact Dataset: Recognition of Activities of Daily Living Using Smartphones, in: International Conference on Information and Communication Technologies for Ageing Well and E-health, Vol. 2, SciTePress, 2016, pp. 143–151. https://doi.org/10.5220/0005792401430151

[22] G. Vavoulas, M. Pediaditis, C. Chatzaki, E. G. Spanakis, M. Tsiknakis, The Mobifall Dataset: Fall

Detection and Classification with A Smartphone, International Journal of Monitoring and Surveillance Technologies Research (IJMSTR), Vol. 2, No. 1, 2014, pp. 44–56. https://doi.org/10.4018/ijmstr.2014010103

[23] J. Reyes-Ortiz, D. Anguita, A. Ghio, L. Oneto, X. Parra, Human Activity Recognition Using Smartphones, UCI Machine Learning Repository, DOI: 10.24432/C54S4K (2012).

[24] E. S. Grood, W. J. Suntay, A Joint Coordinate System for The Clinical Description of Three-Dimensional Motions: Application To The Knee (1983). https://doi.org/10.1115/1.3138397

[25] X. Lin, Y. Li, X. Xie, Y. Ding, X. Wu, C. Ge, SF-CABD: Secure Byzantine Fault Tolerance Federated Learning on Non-IID Data, Knowledge-Based Systems, Vol. 296, 2024, pp. 111851. https://www.sciencedirect.com/science/article/pii/S0950705124004854